

# Low-frequency p- and g-mode solar oscillations

J. Provost, G. Berthomieu, and P. Morel

Département Cassini, UMR CNRS 6529, Observatoire de la Côte d'Azur, B.P. 4229, 06304 Nice CEDEX 4, France

Received 27 July 1999 / Accepted 25 October 1999

**Abstract.** In order to help the detection and identification of low-frequency p- and g-modes in the solar spectrum observed by ground-based networks and SoHO experiments, we study the properties of low degree ( $\ell=0 - 6$ ) low-frequency (100 - 2000  $\mu\text{Hz}$ ) solar oscillations. The frequencies of p- and g-modes have been computed for a set of solar models with updated physics. We point out the specific properties of the oscillations of mixed character, with noticeable amplitude both in central and external layers. We analyze the sensitivity of low-frequency oscillations to solar parameters like age, metallicity and luminosity, and to various physical processes, like convective core overshoot and mass loss during the beginning of solar evolution. We estimate the sensitivity of the splittings of these low-frequency oscillations to the core rotation.

**Key words:** Sun: interior – Sun: oscillations – Sun: rotation

## 1. Introduction

A large number of acoustic frequencies has already been detected in the solar oscillation spectrum, leading to a “seismic” model of the Sun rather close to the actual standard solar models (e.g. Christensen-Dalsgaard et al. 1996, Gough et al. 1996), except for the layers near the surface, below the convection zone and in the deep interior. These observations do not constrain strongly the solar core description and observed frequencies of low degree low-frequency modes, which penetrate deeply into the solar core, are needed. A lot of work has been devoted to low-frequency gravity modes, specially by asymptotic methods (e.g. Ellis 1986, Gabriel 1986, Provost & Berthomieu 1986, Berthomieu & Provost 1991), with the aim of helping their detection and identification in the future helioseismic observations of the experiments on board SoHO. Up to now there are only an upper observational limit from VIRGO (Fröhlich et al. 1998) and possible candidates from GOLF (Gabriel et al. 1998). In this paper we study numerically the properties of low-frequencies modes in an intermediate frequency range from 100 to 2000  $\mu\text{Hz}$ , where they are both g- and p-modes, and the sensitivity of their frequencies to the structure of the solar interior. In

the low part of that frequency range, the g-modes have a spectrum with a large number of peaks, with frequencies satisfying a second order asymptotic law. However for the small degrees ( $\ell \leq 2$ ) the reasonably small number of peaks in the frequency spectrum could make easier the identification of gravity modes. In view of interpretation of experiments like LOI or MDI we consider degree  $\ell$  from 1 to 6. In Sect. 2 we present some specific properties of the low-frequency solar oscillations. In Sect. 3, we describe the set of calibrated solar models that we consider. Finally we estimate in Sects. 4 and 5 the sensitivity of the frequencies and of the splittings of the low frequency oscillations to the solar structure and to the solar core rotation. We find that it is much larger for gravity modes than for acoustic modes.

## 2. Properties of the low-frequency modes

The oscillations in the low-frequency range depend both of the profiles of the sound speed  $c$  and of the Brunt-Väisälä frequency  $N$ :

$$c \sim \sqrt{\frac{\Gamma_1 RT}{\mu}}, \quad N^2 \sim g \left[ \frac{1}{\mu} \frac{d\mu}{dr} + \frac{\delta_T}{T} \left( \left( \frac{dT}{dr} \right)_{\text{ad}} - \frac{dT}{dr} \right) \right] \quad (1)$$

where  $g$  is the gravity,  $T$  the temperature,  $r$  the radius,  $\mu$  the mean molecular weight,  $\delta_T = -\left(\frac{\partial \ln \rho}{\partial \ln T}\right)_P$  and  $\Gamma_1$  the adiabatic exponent. The derivative of the logarithm of the sound speed  $d \ln c/dr$  and the square of the Brunt-Väisälä frequency  $N^2$  contain respectively contributions of the temperature and mean molecular weight gradients. In the envelope, the main contribution comes from the temperature gradient. The mean molecular weight gradient very significantly contributes to the variations of  $d \ln c/dr$  and  $N^2$  in the solar core.

Above the maximum of the Brunt-Väisälä frequency, i.e. about 450  $\mu\text{Hz}$ , we have acoustic modes (p-modes) with frequencies depending principally on the sound speed. Below 200  $\mu\text{Hz}$ , we are dealing with gravity modes (g-modes) whose frequencies depend principally on  $N$  and which are already in the asymptotic range. In between are low radial order g-modes, f-modes (zero radial node) and  $p_1$ -modes (p-modes with one radial node). Some of them have a pronounced mixed character.

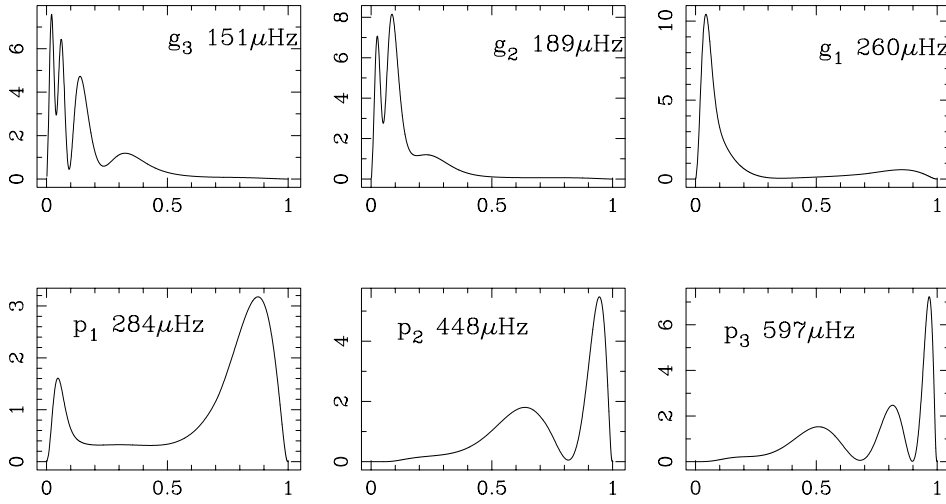


**Fig. 1.** Kinetic energy density (i.e. normalized  $\rho r^2 \delta \mathbf{r} \delta \mathbf{r}^*$  where  $\delta \mathbf{r}$  is the displacement vector) as function of the radius for modes  $g_3$ ,  $g_2$ ,  $g_1$ ,  $p_1$ ,  $p_2$  and  $p_3$  of degree  $\ell=1$  computed for the reference model M1.

**Table 1.** Global characteristics of solar models.  $Z/X$  is the ratio of heavy element to hydrogen content at the photospheric level.  $\zeta_{ov}$  is the overshoot parameter of the early convective core.  $Y_{surf}$  is the helium content of the solar outer layers.  $r_{zc}$  is the location of the lower boundary of the convection zone.  $T_c$ ,  $\rho_c$  and  $Y_c$  are the central temperature, density and helium content.  $\Phi_{Ga}$ ,  $\Phi_{Cl}$  and  $\Phi_{Ka}$  are the predicted capture rates for the three neutrino experiments.  $\delta\nu_{02}$  and  $\delta\nu_{13}$  are characteristic values of the low degree 5 mn p-mode frequency differences  $\Delta\nu_{n,\ell} = \nu_{n,\ell} - \nu_{n-1,\ell+2} = \delta\nu_{\ell\ell+2} + S_\ell(n - n_0)$  for  $\ell=0$  and 1 and  $n_0 = 21$ .  $P_0$  is the characteristic period of low degree gravity modes (see Eq. (5)). The protosolar mass is  $1 M_\odot$ , except for the mass loss model M3 ( $M_p = 1.1 M_\odot$ ).

	M1	M2	M3	M4	M5	M6	M7	M8	$\odot$	
age (Gy)	4.65	4.65	4.65	4.65	4.65	4.75	4.65	4.65		
$Z/X$	0.0245	0.0260	0.0245	0.0245	0.0245	0.0245	0.0245	0.0245		
$\zeta_{ov}$	–	–	–	0.20	0.25	–	–	–		
$Y_{surf}$	0.243	0.247	0.243	0.243	0.243	0.242	0.244	0.248	0.232 – 0.249	
$r_{zc}/R_\odot$	0.712	0.710	0.711	0.712	0.712	0.711	0.711	0.713	$0.713 \pm 0.001$	
$T_c (10^7 \text{K})$	1.571	1.579	1.574	1.572	1.573	1.574	1.563	1.569		
$\rho_c (\text{g cm}^{-3})$	153.8	154.5	156.3	152.9	149.1	155.5	151.4	155.9		
$Y_c$	0.644	0.651	0.652	0.641	0.624	0.650	0.644	0.648		
$\Phi_{Ga} (\text{SNU})$	129	132	130	129	129	130	128	128	$77.75 \pm 6.2^{+4.3}_{-4.7}$	
$\Phi_{Cl} (\text{SNU})$	7.84	8.46	8.01	7.86	7.96	8.04	7.80	7.45	$2.55 \pm 0.23$	
$\Phi_{Ka} (\text{ev day})^{-1}$	0.56	0.61	0.58	0.57	0.57	0.58	0.56	0.55	$0.29 \pm 0.02$	
$\delta\nu_{02} (\mu\text{Hz})$	9.10	9.06	8.96	9.10	9.09	9.01	9.05	8.99	$9.00 \pm 0.04$	LOI
									$9.01 \pm 0.04$	GOLF
$\delta\nu_{13} (\mu\text{Hz})$	15.95	15.88	15.77	15.99	16.13	15.82	15.88	15.81	$15.88 \pm 0.03$	LOI
									$15.71 \pm 0.07$	GOLF
$P_0 (\text{mn})$	35.08	34.94	34.63	35.39	36.74	34.77	35.42	34.73		

### 2.1. Mixed modes in intermediate frequency range

The mixed modes have frequencies in the range 200-450  $\mu\text{Hz}$ . Most of them lie in the region of the avoided crossing of g-modes with the f-mode ridge which is visible in Fig. 1 of Christensen-Dalsgaard & Berthomieu (1991). The particularity of these modes can be related to the properties of their eigenfunctions. As an example, the kinetic energy density of the modes of degree  $\ell=1$  in the intermediate frequency range 200 - 400  $\mu\text{Hz}$  is plotted in Fig. 1. The plots of the first line concern gravity modes which have their amplitude concentrated in the solar core ( $r \lesssim 0.2R_\odot$ ). In the two last graphs are represented two p-modes with amplitude in the solar envelope ( $r \gtrsim 0.75R_\odot$ ). The mode  $p_1$  has a mixed character, intermediate between p-and g-modes, with amplitude both in the envelope like a p-mode and in the core like a g-mode. Examples of eigenfunctions for these

mixed modes are shown in Fig. 2 for  $p_1$  modes of degree  $\ell=1$  and 2 and  $g_5$  mode of degree  $\ell=6$ . These eigenfunctions are given for different solar models described in Sect. 3 and are rather sensitive to the model. One has also modes of mixed character in the gravity mode range, respectively for ( $\ell=3, n=4, \nu \sim 239 \mu\text{Hz}$ ), ( $\ell=4, n=5, \nu \sim 251 \mu\text{Hz}$ ), ( $\ell=5, n=5, \nu \sim 272 \mu\text{Hz}$ ). Unlike the other g-modes, the mixed modes have a larger amplitude near the surface, which makes them interesting for observers. In contrast, the intermediate mode between p- and g-modes with zero radial order, i.e. the f-mode, has a large amplitude at the surface for degrees larger than about 20 (Christensen-Dalsgaard & Berthomieu 1991), but it has a maximum amplitude in the core for smaller degrees, like a g-mode, as illustrated in Fig. 3 for  $\ell=6$ .

The mixed character of some modes appears in the range 200-400  $\mu\text{Hz}$  also very clearly in Fig. 4 (upper panel), which

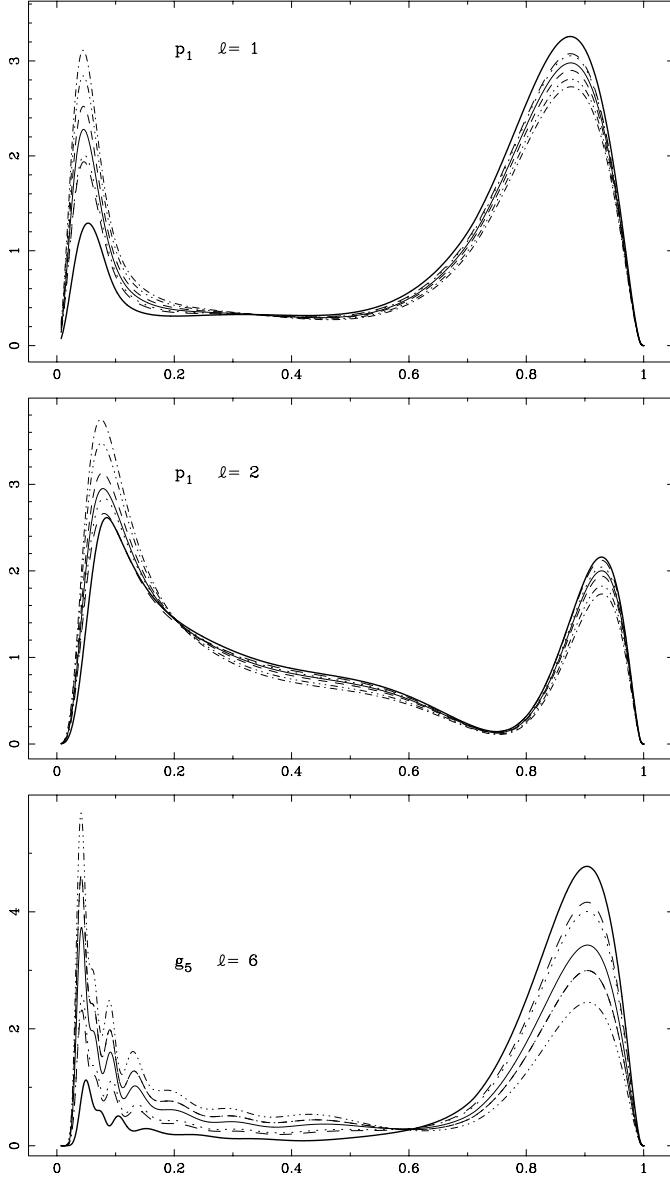


**Fig. 2.** Kinetic energy density as function of the radius for the  $p_1$  mode of degree  $\ell=1$  (upper panel), the  $p_1$  mode of degree  $\ell=2$  (middle panel) and the  $g_5$  mode of degree  $\ell=6$  (lower panel), for different solar models. (M1 full; M2 dashed; M3 dot-dash; M4 dotted; M6 dot-dot-dot-dash; M7 dashed heavy line; M5 full heavy line).

represents the kinetic energy of the modes equal to  $\omega^2$  times their normalized inertia  $\mathcal{E}_{n,\ell}$ , with:

$$\mathcal{E}_{n,\ell} = \frac{4\pi}{M_\odot} \frac{\int_0^{R_\odot} \rho [\xi_r^2 + \ell(\ell+1)\xi_h^2] dv}{[\xi_r^2(R_{\text{phot}}) + \ell(\ell+1)\xi_h^2(R_{\text{phot}})]}, \quad (2)$$

as a function of the frequency.  $\xi_r$  and  $\xi_h$  are the radial and horizontal displacements and the normalization is taken at the photospheric level, which corresponds to the effective temperature level. The modes of mixed character have smaller energy than the adjacent modes. This means that they will be more easily excited and if we assume equipartition of the energy in the modes, they will exhibit larger surface amplitude than their

neighbors in the spectrum. For example, the energy of the modes of degree  $\ell=5$  and 6 around  $280 \mu\text{Hz}$  is of the same order of magnitude than the one of the first g-modes of degree  $\ell=1, 2, 3$ , which, according to Kumar et al. (1996), are predicted to have a surface amplitude of  $0.1 \text{ mm s}^{-1}$ . Thus, if there is equipartition of energy, these modes  $\ell=5$  and 6 will have the same amplitude at the surface and are possible candidates to be detected in the low-frequency power spectrum.

The frequencies of the oscillation modes can be expressed using a variational principle. In the Cowling's approximation and neglecting surface terms it can be written:

$$\left(\frac{\nu}{2\pi}\right)^2 = \frac{\int (p'p'^*/(\Gamma_1 p) + N^2 \rho \delta \mathbf{r} \cdot \delta \mathbf{r}^*) dv}{\mathcal{E}_{n,\ell}} \equiv \frac{(\mathcal{I}_1 + \mathcal{I}_2)}{\mathcal{E}_{n,\ell}} \quad (3)$$

The quantities  $\mathcal{I}_1$  and  $\mathcal{I}_2$  correspond to the contributions of pressure and buoyancy forces and reflect the respective influence of the sound speed and of the Brunt-Väisälä frequency on the mode frequency. Either  $\mathcal{I}_1$  or  $\mathcal{I}_2$  dominates respectively in the high (p-modes) and low (g-modes) frequency range. Fig. 4 (lower panel) shows the variation of  $\mathcal{I}_2/(\mathcal{I}_1 + \mathcal{I}_2)$  for the modes of our reference model M1. As expected, it appears that for pure p- or g-modes, there is a dominant contribution to the frequency either of the acoustic term  $\mathcal{I}_1$  or of the gravity term  $\mathcal{I}_2$ . In contrast, between 200 and  $450 \mu\text{Hz}$ , the frequency of some modes, specially the g-modes near the avoided crossing with the surface f-mode ridge, is defined by two comparable contributions.

## 2.2. Low-frequency range

The frequencies of modes for  $\nu < 200 \mu\text{Hz}$  can be described by an asymptotic approximation (Tassoul 1980). For sufficiently small frequency, the second order asymptotic period  $P_{n,\ell} = 1/\nu_{n,\ell}$  is given by:

$$P_{n,\ell} \sim \frac{P_0}{\sqrt{\ell(\ell+1)}} (n + \ell/2 + \vartheta) + \frac{P_0}{P_{n,\ell}} \left[ V_1 + \frac{V_2}{\ell(\ell+1)} \right] \quad (4)$$

$$\text{with } P_0 = 2\pi^2 / \int_0^{r_{\text{zc}}} (N/r) dr$$

$$\text{and } V_1 = \lim_{\epsilon \rightarrow 0} \left( \int_\epsilon^{r_{\text{zc}}} \frac{1}{rN} dr - \frac{1}{N(\epsilon)} \right). \quad (5)$$

$\vartheta$  is a phase factor sensitive to the properties of the layers lying below the convection zone (Provost & Berthomieu 1986). The second order coefficient  $V_1$  depends on the Brunt-Väisälä frequency.  $V_2$  depends in a more complex way on the stratification and its expression can be obtained from Berthomieu & Provost (1991). Thus the frequency of g-modes is closely related to the Brunt-Väisälä frequency. Hence the relative frequency difference of two modes of same degree  $\ell$  and same radial order  $n$  corresponding to two different models, is equal to:

$$\frac{\delta\nu}{\nu} \sim -\frac{\delta P_0}{P_0} - (\nu P_0)^2 \frac{[\delta V_1 + \delta V_2/(\ell(\ell+1))]}{P_0} \quad (6)$$

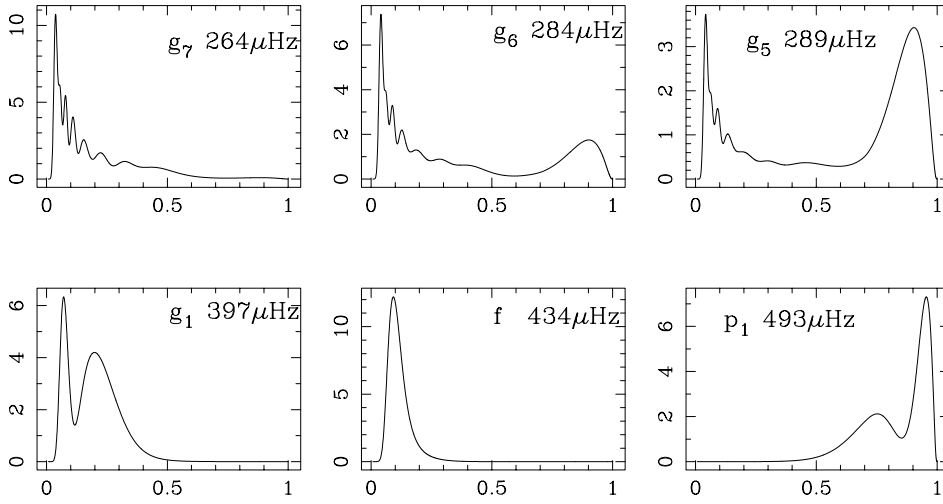


**Fig. 3.** Same as in Fig. 1 for the modes  $g_7$ ,  $g_6$ ,  $g_5$ ,  $g_1$ ,  $f$  and  $p_1$  of degree  $\ell=6$ . The  $g_5$ -mode, close to avoided crossing, has a mixed character. The  $f$ -mode behaves physically as the lowest order trapped  $g$ -mode.

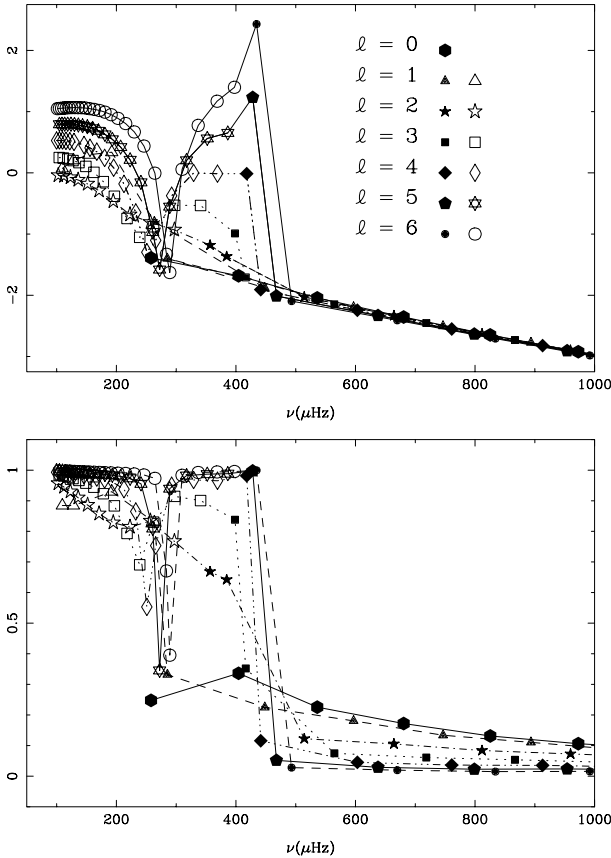


**Fig. 4.** *Upper panel:* Logarithm of the energy  $\omega^2 \mathcal{E}_{n,\ell}$  of the modes for model M1 as a function of the frequency, for modes of degree  $\ell=0, 1, 2, 3, 4, 5$  and  $6$ . The transition from p- to g-modes around  $450 \mu\text{Hz}$  and the existence of a set of modes of mixed character around  $280 \mu\text{Hz}$  is well visible (full symbols for f- and p-modes, open symbols for g-modes). *Lower panel:* Relative contribution of the buoyancy to the frequency, measured as  $\mathcal{I}_2 / (\mathcal{I}_1 + \mathcal{I}_2)$ .  $\mathcal{I}_1$  and  $\mathcal{I}_2$  are defined in Eq. (3).

### 3. On the solar models

We have computed a set of calibrated solar models with updated physics and with some physical processes which are likely to

be present in the Sun, like microscopic diffusion, penetrative convection and mass loss (Morel et al. 1997 (hereafter MPB), Morel et al. 1998b), in order to study the sensitivity of low degree low-frequency modes to the solar structure. Table 1 shows the global characteristics of these models and some properties of their core. All the models include the microscopic diffusion of the chemical elements. The physics is the same as in MPB (OPAL opacity and equation of state), but the nuclear reaction rates are the revised values from Adelberger et al. (1998), except for model M7 computed with the values of Caughlan & Fowler (1988).

Model M1 is the actual reference model. All the models have been calibrated at the solar radius and luminosity ( $R_\odot = 6.9599 \cdot 10^{10} \text{ cm}$ ,  $L_\odot = 3.846 \cdot 10^{33} \text{ erg s}^{-1}$ ; Christensen-Dalsgaard et al. 1996) for a solar age  $t_\odot = 4.65 \text{ Gy}$  and a photospheric metallicity  $Z/X = 0.0245$  (Grevesse & Noels, 1993), except the models M2 ( $Z/X = 0.0260$ ) and M6 ( $t_\odot = 4.75 \text{ Gy}$ ). The solar age is within its seismic estimation (Dziembowski et al. 1999). Models M3 and M8 present a mass loss of  $\dot{M} = -5 \cdot 10^{-10} M_\odot \text{ y}^{-1}$  occurring during the beginning of the evolution, during 200 My, with an additional turbulent mixing below the convection zone for model M8, according to Montalban & Schatzman (1999). The presence of such a mixing is suggested by the discrepancy between solar and model sound speeds, pointed out by the helioseismic inversion (Gough et al. 1996, Richard et al. 1996, Brun et al. 1998, Morel et al. 1998a). Models M4 and M5 include some overshoot of the convective elements at the boundary of the convective core which appears at the end of the pre-main sequence solar evolution, due to the burning of  $^{12}\text{C}$  into  $^{14}\text{N}$  (e.g. Kippenhahn & Weigert 1991). We assume an overshoot of  $\zeta_{\text{ov}} \min(H_p, r_{\text{cv}})$  where  $H_p$  is the pressure scale height and  $r_{\text{cv}}$  the radius of the convective core. The overshoot parameter  $\zeta_{\text{ov}}$  is respectively equal to 0.2 and 0.25 for models M4 and M5.

Table 1 also shows the helium content and lower location of the convection zone, central values of temperature, density and helium content. We give also the values of physical quantities sensitive to the core structure, like the predicted neutrino capture rates for the three neutrino experiments and the small frequency

separation of low degree 5mn p-modes  $\delta\nu_{02}$  and  $\delta\nu_{13}$ . For the predicted neutrino capture rates, the absorption cross sections have been taken from Bahcall et al. (1996) and Bahcall (1997). The observed values of neutrino fluxes (Hempel et al. 1999, Davis 1994 and Fukuda et al. 1996) and the helium content (Basu 1997) and location of the lower boundary of the convection zone (Basu & Antia 1995) derived by inversion of the observations are given in the last column. The quantities  $\delta\nu_{02}$  and  $\delta\nu_{13}$  are characteristic values of the low degree p-mode frequency differences obtained by fitting the numerical frequency differences:

$$\Delta\nu_{n,\ell} \equiv \nu_{n,\ell} - \nu_{n-1,\ell+2} = \delta\nu_{\ell\ell+2} + S_{\ell}(n - n_0) \quad (7)$$

for  $\ell=0$  and 1,  $n_0=21$  and  $\nu$  from 2.5 to 4.1 mHz, which provide information on the properties of the core of the Sun. The solar values are estimated from the observations of VIRGO/LOI (Fröhlich et al. 1997) and GOLF (Lazrek et al. 1997)

Fig. 5 shows the comparison of the sound speed of these models to that of the solar seismic model obtained by inversion of the observed frequencies of p-modes in the five minute frequency range (Turck-Chièze et al., 1997). The agreement is within some  $10^{-3}$  for all the models in the radius range 0.1 to  $0.9 R_{\odot}$ . Model M5, which has the largest core overshoot parameter, differs strongly below  $0.05 R_{\odot}$ , which is a region where the inversion of solar frequencies does not give reliable results. The surface, a thin layer just below the convection zone and particularly the solar core are the regions which differ mostly from the models. Note that the additional mixing below the convection zone included in model M8 leads to a local increase of the sound speed, thus model M8 is closer to the seismic model than M1.

Fig. 6 shows the relative differences of  $c$  and  $N$  as functions of radius, between the models of Table 1 and the reference model M1. Both  $\delta c/c$  and  $\delta N/N$  are due to changes of gradient of  $\mu$  in the nuclear core ( $r < 0.2 R_{\odot}$ ) and to changes of temperature gradient outside. It is shown that  $\delta N/N$  is larger than  $\delta c/c$  by an order of magnitude and that the differences in  $\delta N/N$  have large amplitude in the core. Note the large central differences both in  $c$  and  $N$  for the model M5 with the overshoot parameter  $\zeta_{ov}=0.25$ , which corresponds to the large difference of sound speed in the core between the Sun and the model (Fig. 5). The increase of the overshoot parameter increases the amount of  $^{12}\text{C}$  available for burning into  $^{14}\text{N}$ . This induces a larger early solar convective core, which lasts longer. As a result at solar age, the deep structure and the oscillation frequencies which are sensitive to the solar core vary strongly non linearly with the overshoot parameter. If progress in the determination of sound speed from helioseismic data confirm the small sound speed difference between the Sun and the reference model down to the solar center, then an overshoot parameter of 0.25 should be ruled out.

#### 4. Sensitivity of low-frequency modes to solar structure

The frequencies of the set of models described in Sect. 3 have been computed for the gravity and pressure modes with degrees

$\ell=0$  to 6 and frequencies from 100 to 2000  $\mu\text{Hz}$ . Table 2 gives the frequencies and inertia for these modes of the reference model M1. The results on the sensitivity of the frequencies to the parameters of the solar model (age, metallicity and luminosity) and to the physics (nuclear reaction rates, overshoot, mass loss and mass loss with additional mixing) are given in Figs. 7, 8 and 9. They represent the relative frequency differences  $\delta\nu/\nu$ , between the frequencies of different pairs of solar models. In a previous paper (Provost et al. 1998) it has been shown that the frequencies in the low-frequency range are higher for a model with microscopic diffusion than for a standard one, with differences up to 10  $\mu\text{Hz}$  around 300  $\mu\text{Hz}$  and of order 2  $\mu\text{Hz}$  in p-mode range (see Fig. 3 of Provost et al. 1998).

According to the physical nature of the modes, as described in Sect. 2, Figs. 7, 8 and 9 show that three frequency domains may be distinguished.

1. Above the maximum of the Brunt-Väisälä frequency, about 450  $\mu\text{Hz}$ , the oscillations are acoustic p-modes with frequencies depending principally on the sound speed. In this frequency range, the frequency differences between two models are very small,
2. Below 200  $\mu\text{Hz}$ , one has gravity g-modes which frequencies depend principally on  $N$  and which are already in the asymptotic range. In these two regions the differences are almost independent of the degree.
3. In between are low radial order g-modes, f-modes (zero radial node) and  $p_1$ -modes (p-modes with one radial node), including modes with mixed character.

Fig. 2 shows the great sensitivity of the eigenfunctions to the modifications introduced in the solar models is shown for  $p_1$ -modes of degree  $\ell=1$  and 2. Note that in contrast to the large sensitivity of the eigenfunctions of the mixed modes, their frequencies are less sensitive than those of the adjacent modes. This is due to a balance between the respective contributions of the relative differences of sound speed and Brunt-Väisälä frequency to the difference of eigenfrequencies.

##### 4.1. Effects of changing the solar model

Fig. 8 shows respectively the sensitivity of low-frequency spectrum to the age, the photospheric metallicity measured by the ratio of heavy elements to hydrogen content  $Z/X$  and the luminosity at solar age. The frequencies increase with age, metallicity  $Z/X$  and luminosity. As a result we find that either a change of 1% in age or a change of 6% in metallicity increases the low-frequencies by about 0.4%. Work in progress announced by Grevesse & Sauval (1998) seems to indicate a smaller revised value of the solar metallicity. If confirmed such a decrease of  $Z/X$  would decrease slightly the predicted neutrino flux but increase the characteristic 5mn p-mode separation  $\delta\nu_{02}$  out of the observed range. The effect of a slightly larger luminosity by 3.5%, which corresponds to the upper value reported in Guenther et al. (1992), is an increase of the g-mode frequencies by 0.2%.

**Table 2.** Frequency  $\nu_{n,\ell}$  and inertia  $\mathcal{E}_{n,\ell}$  of low frequency modes for the reference model M1.

	$\nu_{n,\ell}$	$\mathcal{E}_{n,\ell}$	$\nu_{n,\ell}$	$\mathcal{E}_{n,\ell}$	$\nu_{n,\ell}$	$\mathcal{E}_{n,\ell}$	$\nu_{n,\ell}$	$\mathcal{E}_{n,\ell}$
	$\ell=0$		$\ell=1$		$\ell=2$		$\ell=3$	
g10	—	—	—	—	102.80	$8.56 \cdot 10^{-1}$	137.33	$7.75 \cdot 10^{-1}$
g9	—	—	—	—	112.06	$7.02 \cdot 10^{-1}$	148.88	$5.73 \cdot 10^{-1}$
g8	—	—	—	—	122.99	$5.53 \cdot 10^{-1}$	162.33	$3.86 \cdot 10^{-1}$
g7	—	—	—	—	136.03	$4.11 \cdot 10^{-1}$	178.12	$2.26 \cdot 10^{-1}$
g6	—	—	—	—	151.78	$2.85 \cdot 10^{-1}$	196.63	$1.07 \cdot 10^{-1}$
g5	—	—	109.49	$9.81 \cdot 10^{-1}$	171.06	$1.74 \cdot 10^{-1}$	217.77	$3.77 \cdot 10^{-2}$
g4	—	—	128.13	$9.74 \cdot 10^{-1}$	194.72	$9.98 \cdot 10^{-2}$	238.98	$1.54 \cdot 10^{-2}$
g3	—	—	153.72	$8.33 \cdot 10^{-1}$	222.70	$4.16 \cdot 10^{-2}$	262.08	$1.91 \cdot 10^{-2}$
g2	—	—	192.25	$5.87 \cdot 10^{-1}$	256.88	$2.35 \cdot 10^{-2}$	297.45	$3.32 \cdot 10^{-2}$
g1	—	—	263.54	$2.29 \cdot 10^{-2}$	297.01	$1.32 \cdot 10^{-2}$	340.88	$2.51 \cdot 10^{-2}$
f	—	—	—	—	356.71	$5.15 \cdot 10^{-3}$	398.40	$6.43 \cdot 10^{-3}$
p1	257.88	$6.11 \cdot 10^{-3}$	285.27	$4.89 \cdot 10^{-3}$	384.54	$2.90 \cdot 10^{-3}$	416.42	$1.13 \cdot 10^{-3}$
p2	404.45	$1.27 \cdot 10^{-3}$	448.31	$6.55 \cdot 10^{-4}$	514.38	$3.54 \cdot 10^{-4}$	564.62	$2.22 \cdot 10^{-4}$
p3	536.04	$3.14 \cdot 10^{-4}$	596.83	$1.79 \cdot 10^{-4}$	664.27	$1.05 \cdot 10^{-4}$	718.39	$6.80 \cdot 10^{-5}$
p4	680.60	$9.49 \cdot 10^{-5}$	746.54	$5.60 \cdot 10^{-5}$	811.68	$3.56 \cdot 10^{-5}$	866.84	$2.47 \cdot 10^{-5}$
p5	825.41	$3.29 \cdot 10^{-5}$	893.56	$2.10 \cdot 10^{-5}$	959.73	$1.37 \cdot 10^{-5}$	1014.91	$9.61 \cdot 10^{-6}$
p6	972.73	$1.26 \cdot 10^{-5}$	1039.43	$8.37 \cdot 10^{-6}$	1105.01	$5.74 \cdot 10^{-6}$	1161.53	$4.12 \cdot 10^{-6}$
p7	1118.09	$5.32 \cdot 10^{-6}$	1185.44	$3.60 \cdot 10^{-6}$	1250.59	$2.46 \cdot 10^{-6}$	1306.66	$1.78 \cdot 10^{-6}$
p8	1263.47	$2.29 \cdot 10^{-6}$	1329.51	$1.58 \cdot 10^{-6}$	1394.49	$1.09 \cdot 10^{-6}$	1450.86	$7.81 \cdot 10^{-7}$
p9	1407.48	$1.01 \cdot 10^{-6}$	1472.76	$6.89 \cdot 10^{-7}$	1535.74	$4.82 \cdot 10^{-7}$	1591.28	$3.54 \cdot 10^{-7}$
p10	1548.35	$4.50 \cdot 10^{-7}$	1612.42	$3.17 \cdot 10^{-7}$	1674.37	$2.28 \cdot 10^{-7}$	1728.92	$1.74 \cdot 10^{-7}$
	$\ell=4$		$\ell=5$		$\ell=6$			
g10	167.24	$7.88 \cdot 10^{-1}$	193.12	$9.44 \cdot 10^{-1}$	215.51	1.37		
g9	180.31	$5.37 \cdot 10^{-1}$	207.09	$6.12 \cdot 10^{-1}$	229.91	$8.80 \cdot 10^{-1}$		
g8	195.33	$3.16 \cdot 10^{-1}$	222.96	$3.27 \cdot 10^{-1}$	246.10	$4.51 \cdot 10^{-1}$		
g7	212.70	$1.45 \cdot 10^{-1}$	241.07	$1.20 \cdot 10^{-1}$	264.36	$1.41 \cdot 10^{-1}$		
g6	232.40	$4.15 \cdot 10^{-2}$	260.91	$1.58 \cdot 10^{-2}$	283.75	$5.79 \cdot 10^{-3}$		
g5	250.93	$7.99 \cdot 10^{-3}$	272.33	$3.53 \cdot 10^{-3}$	289.36	$2.79 \cdot 10^{-3}$		
g4	265.77	$1.11 \cdot 10^{-2}$	289.21	$3.34 \cdot 10^{-2}$	309.85	$1.18 \cdot 10^{-1}$		
g3	292.38	$4.93 \cdot 10^{-2}$	317.43	$1.59 \cdot 10^{-1}$	336.90	$5.24 \cdot 10^{-1}$		
g2	329.17	$9.16 \cdot 10^{-2}$	352.02	$2.94 \cdot 10^{-1}$	368.52	1.09		
g1	369.13	$7.09 \cdot 10^{-2}$	386.39	$2.99 \cdot 10^{-1}$	397.51	1.57		
f	417.98	$5.53 \cdot 10^{-2}$	428.05	$9.31 \cdot 10^{-1}$	434.50	$1.4210^{+1}$		
p1	441.54	$6.31 \cdot 10^{-4}$	467.68	$4.42 \cdot 10^{-4}$	493.04	$3.29 \cdot 10^{-4}$		
p2	603.13	$1.56 \cdot 10^{-4}$	637.71	$1.15 \cdot 10^{-4}$	669.89	$8.64 \cdot 10^{-5}$		
p3	761.03	$4.83 \cdot 10^{-5}$	798.80	$3.63 \cdot 10^{-5}$	834.07	$2.80 \cdot 10^{-5}$		
p4	913.04	$1.80 \cdot 10^{-5}$	954.13	$1.36 \cdot 10^{-5}$	992.06	$1.05 \cdot 10^{-5}$		
p5	1061.99	$7.19 \cdot 10^{-6}$	1104.69	$5.55 \cdot 10^{-6}$	1144.75	$4.36 \cdot 10^{-6}$		
p6	1210.40	$3.07 \cdot 10^{-6}$	1254.37	$2.35 \cdot 10^{-6}$	1295.32	$1.84 \cdot 10^{-6}$		
p7	1356.13	$1.34 \cdot 10^{-6}$	1401.34	$1.03 \cdot 10^{-6}$	1443.44	$7.97 \cdot 10^{-7}$		
p8	1500.16	$5.83 \cdot 10^{-7}$	1545.03	$4.50 \cdot 10^{-7}$	1587.08	$3.55 \cdot 10^{-7}$		
p9	1640.62	$2.70 \cdot 10^{-7}$	1685.58	$2.13 \cdot 10^{-7}$	1727.48	$1.72 \cdot 10^{-7}$		
p10	1777.72	$1.39 \cdot 10^{-7}$	1822.92	$1.15 \cdot 10^{-7}$	1865.63	$9.70 \cdot 10^{-8}$		

Concerning the sensitivity of the low-frequency oscillations to the physics, we first studied the sensitivity to updated nuclear physics. The effect on global parameters of introducing updated nuclear reaction rates can be seen from the comparison of models M1 and M7 (Table 1): it results a slightly higher central temperature, hence higher predicted neutrinos capture rates and p-modes small separation (see Morel et al. 1999 for details). The frequency differences between model M1 and model M7 are plotted in Fig. 7 for degrees  $\ell=0$  to 6. The low-frequencies are increased by these updated parameters up to  $3.5 \mu\text{Hz}$ . The

almost linear behavior of the frequency differences  $\delta\nu$  and of the relative frequency differences  $\delta\nu/\nu$  with the frequency is expected from the asymptotic formulas (4) and (6), as detailed in the next subsection (Sect. 4.2).

Models with an overshoot of the convective core lead to lower g-mode frequencies than for the reference model. For model M4 with an overshoot of  $\zeta_{\text{ov}}=0.2$ , the low-frequencies are decreased by an amount up to  $4 \mu\text{Hz}$ , as seen in Fig. 8, while the p-mode are almost not modified. We have also studied the effect of a mass loss of  $0.1 M_{\odot}$  occurring during the first stage

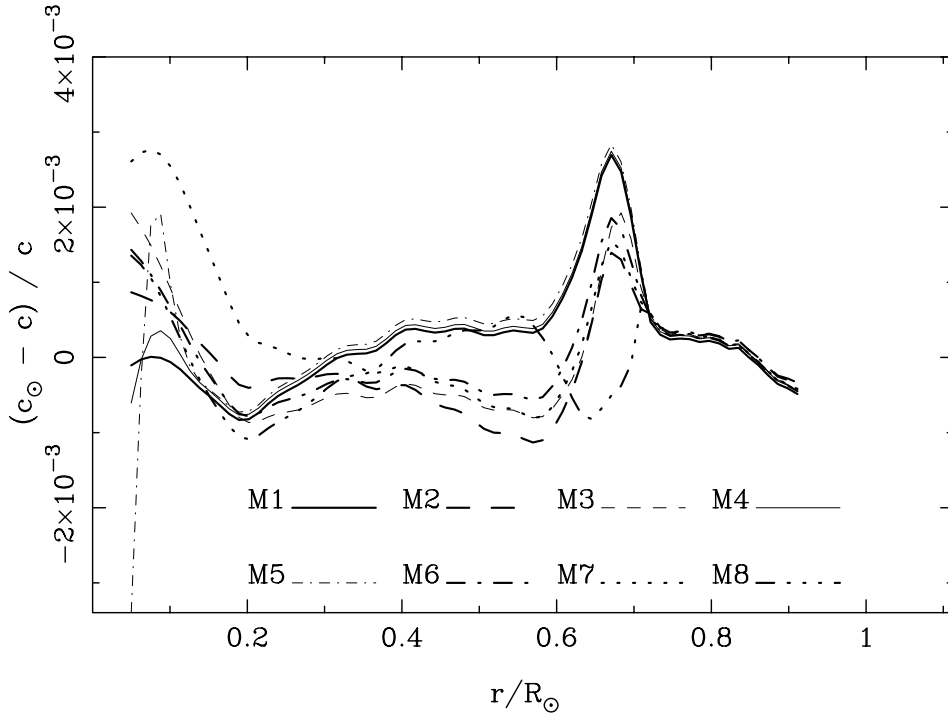


**Fig. 5.** Relative difference in sound speed between the Sun and the models of Table 1.

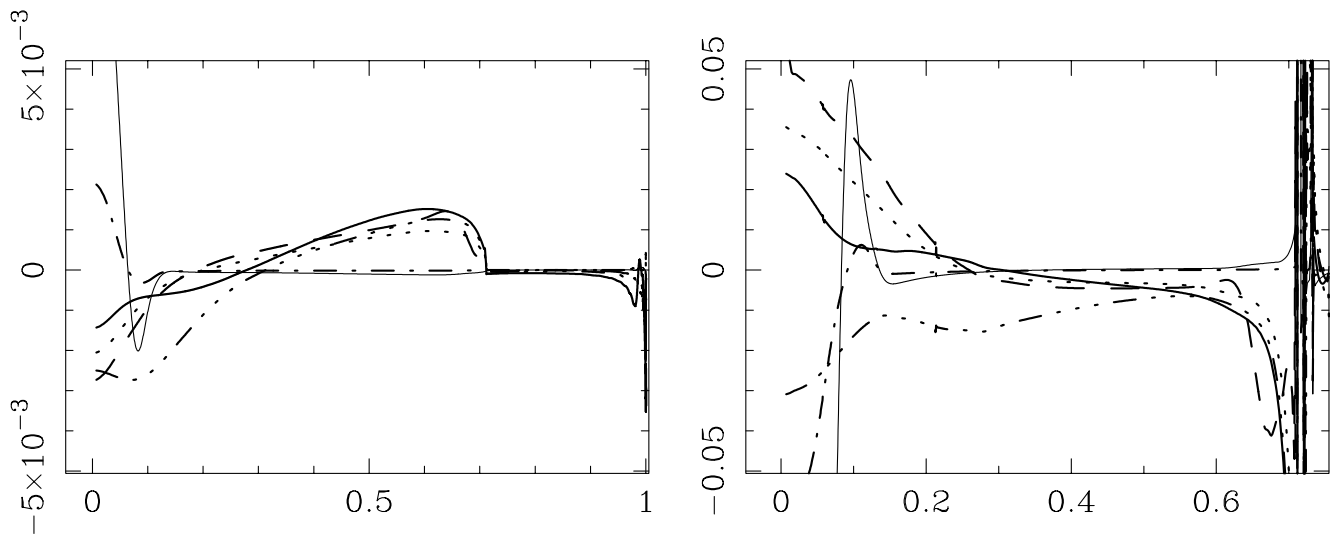


**Fig. 6.** *Left:* Relative difference of the sound speed  $c$  between different solar models and the reference model M1. (M2 - M1 full (metallicity); M3 - M1 dashed (strong mass loss rate); M4 - M1 dot-dashed (core overshoot  $\zeta_{ov}=0.2$ ); M6 - M1 dotted (age); M7 - M1 dash-dot-dot-dot (updated nuclear data); M5 - M1 thin line (core overshoot  $\zeta_{ov}=0.25$ ). *Right:* Relative difference of the Brunt-Väisälä frequency  $N$ .

of evolution. The low frequencies are increased by an amount which depends on the mass loss rate. The strong mass loss rate considered here results in a smaller change of the solar structure, hence of the solar oscillations frequencies (Fig. 8 middle panel). A mild mass loss rate, not presented here, would increase the frequencies up to  $4 \mu\text{Hz}$  but is not compatible with the p-modes properties (Guzik & Cox 1991, MPB). Finally we show in Fig. 8 (lower panel) the relative frequency differences between model M8 and the reference model M1. Let us recall that M8 is computed with a strong mass loss rate and with additional mixing below the convection zone, which makes the

sound speed of this model very close to the seismic Sun. These relative frequency differences are slightly smaller than in the case without additional mixing.

#### 4.2. Low-frequency range

The frequency differences between two models vary almost linearly in g-mode range below  $200 \mu\text{Hz}$ . The almost linear behavior in Fig. 7 (upper panel) at low frequency corresponds to the first order approximations of relations (4) and (6). The slope measured in Fig. 7 in the low frequency range corresponds well

**Table 3.** Sensitivity of the second order coefficients of the period of the gravity modes to the model:  $\delta P_0/P_0$ ,  $\delta V_1/P_0$  and  $\delta V_2/P_0$  are the differences between the considered model and the reference model M1, obtained by least square fit of  $\delta\nu/\nu$  according the relation (6).  $P_0=35.08$  mn.

	M2	M3	M4	M5	M6	M7	M8
$\delta P_0/P_0$	-0.0041	-0.0127	0.0089	0.045	-0.0087	0.0097	0.0105
$\delta V_1/P_0$	$8.97 \cdot 10^{-4}$	$2.88 \cdot 10^{-3}$	$-6.12 \cdot 10^{-3}$	$-3.40 \cdot 10^{-2}$	$1.91 \cdot 10^{-3}$	$-4.08 \cdot 10^{-3}$	$-3.2 \cdot 10^{-3}$
$\delta V_2/P_0$	$2.40 \cdot 10^{-2}$	$7.24 \cdot 10^{-2}$	$-4.44 \cdot 10^{-2}$	$-1.62 \cdot 10^{-1}$	$4.65 \cdot 10^{-2}$	$-3.87 \cdot 10^{-2}$	$-7.6 \cdot 10^{-2}$
$\delta V_2/\delta V_1$	26.78	25.14	7.25	4.9	24.34	9.48	23.75

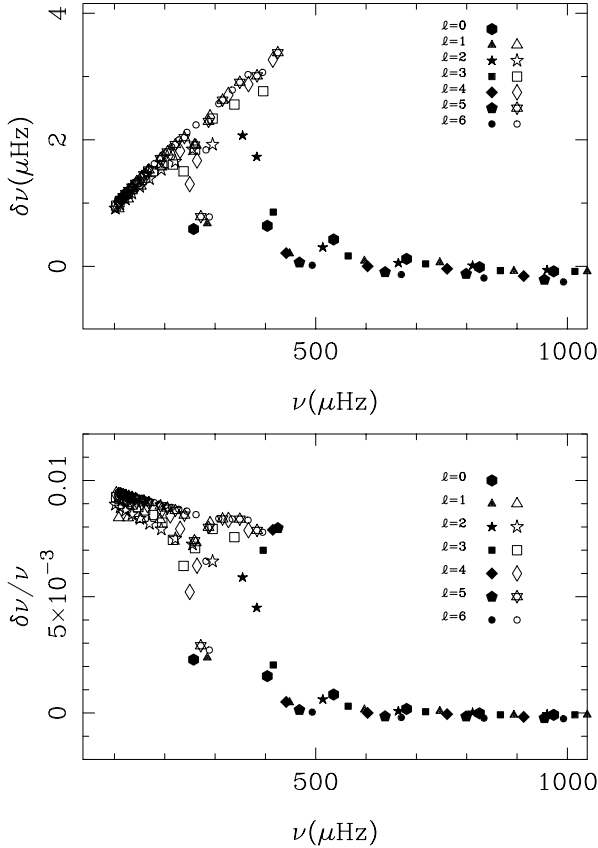


**Fig. 7.** Effect of updated nuclear reaction rates. *Upper panel:* Difference of the frequencies of g-modes (open symbols) and low-frequency f- and p-modes (full symbols) between the models M1 with updated and M7 with Caughlan & Fowler nuclear reaction rates (M1 - M7), for modes of degree  $\ell=0, 1, 2, 3, 4, 5, 6$ . *Lower panel:* Relative frequency differences. Note that the frequencies of the three non radial mixed modes around  $280 \mu\text{Hz}$  for  $\ell=1, 2, 6$  are rather insensitive to the considered change of nuclear reaction rates.

to the relative differences of the characteristic periods  $P_0$  of the gravity modes for the models (Table 1). Its sign is in agreement with the signs of the corresponding relative variations of  $\delta N/N$  in the core plotted in Fig. 6. The departure from first order is more visible in the lower panel of Fig. 7 and in Figs. 8 and 9. Using the relation (6), we have fitted the frequency differences for modes of frequency  $\nu$  less than  $200 \mu\text{Hz}$  considering only modes with radial order larger than 4 and with degrees from 2 to 6. Thus we have estimated the coefficients which charac-

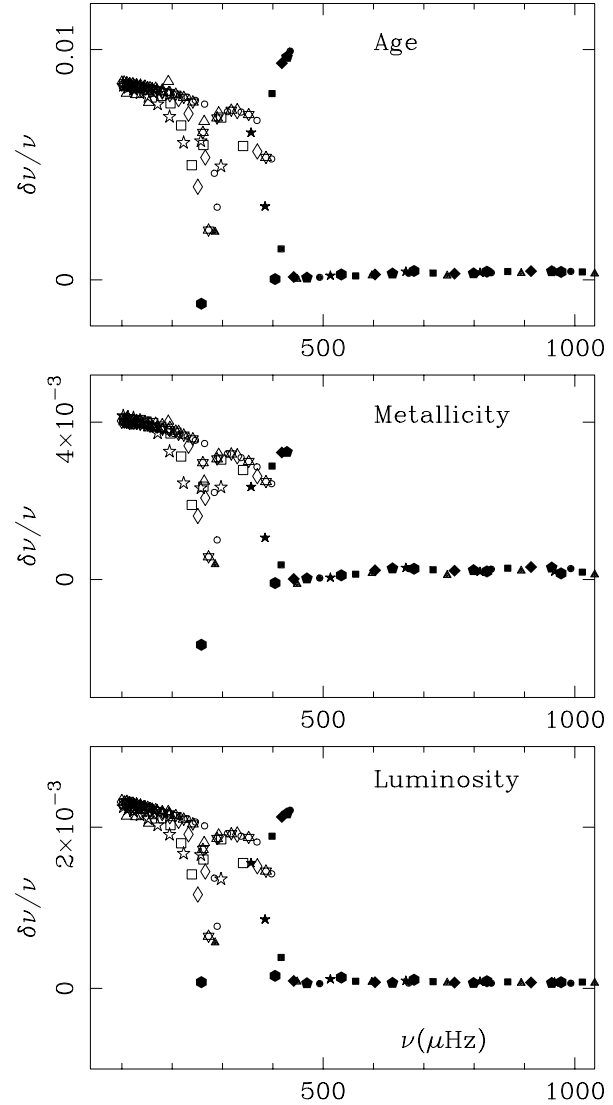


**Fig. 8.** Relative frequency differences of low-frequency modes  $\delta\nu/\nu$  as a function of the frequency (in  $\mu\text{Hz}$ ) between a solar model and the reference model M1 to test the sensitivity to the solar parameters: age (M6), metallicity (M2) and luminosity. Symbols of Fig. 7 are used.

terise the departure from first order, i.e. the quantities  $\delta P_0/P_0$ ,  $\delta V_1/P_0$  and  $\delta V_2/P_0$  between the two considered models. Results are given in Table 3. The value obtained by the second order fit of  $\delta\nu/\nu$  are in a very good agreement with the values of  $\delta P_0/P_0$  directly computed from the models (Table 1). For



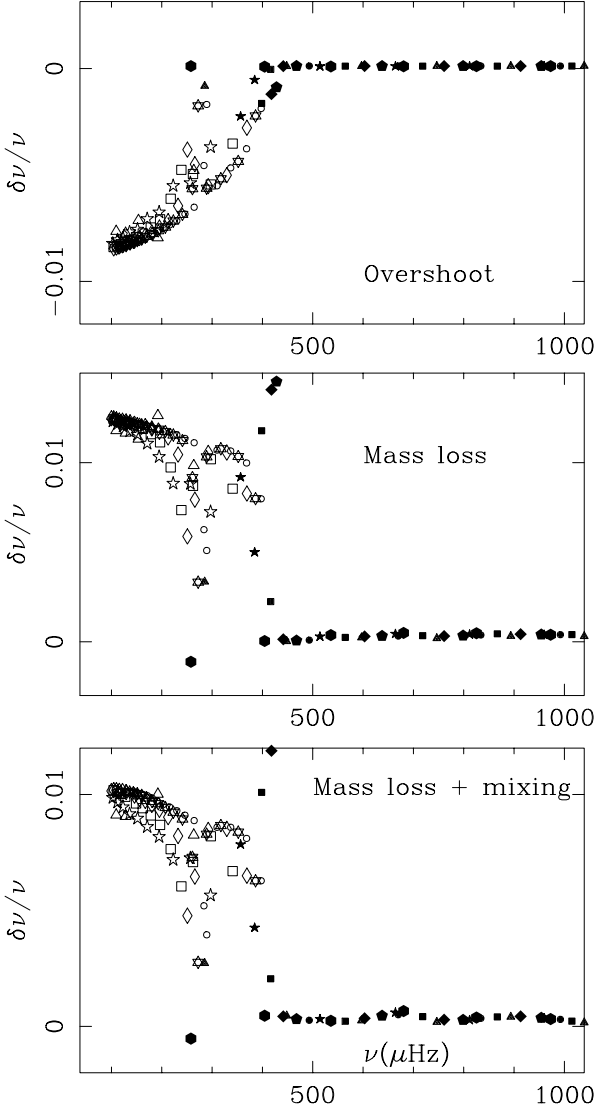


**Fig. 9.** Relative frequency differences of low-frequency modes  $\delta\nu/\nu$  as a function of the frequency (in  $\mu\text{Hz}$ ) between a solar model and the reference model M1 to test the sensitivity to the following physical processes: overshoot (M4), strong mass loss rate (M3) and mass loss and additional turbulent mixing (M8). Symbols of Fig. 7 are used.

the solar models, considered here, a decrease of  $P_0$  is related to an increase of the second order parameters  $\delta V_1$  and  $\delta V_2$ . We note that  $\delta V_2/\delta V_1$  is of order 25, except for the models with core overshoot M4 and M5 and the model M7 with the Caughlan & Fowler nuclear reaction rates. These results provide a range of parameters of the asymptotic formula which could be useful to search g-modes below  $200 \mu\text{Hz}$ .

### 5. Rotational splittings in low-frequency range

The solar rotation induces a splitting of each frequency  $\nu_{n,\ell}$  into  $2\ell+1$  separate frequencies  $\nu_{n,\ell,m}$ , where  $m$  is the azimuthal order of the oscillation. We define the splitting as:

$$\sigma_{n,\ell,m} = (\nu_{n,\ell,m} - \nu_{n,\ell,-m})/2m.$$

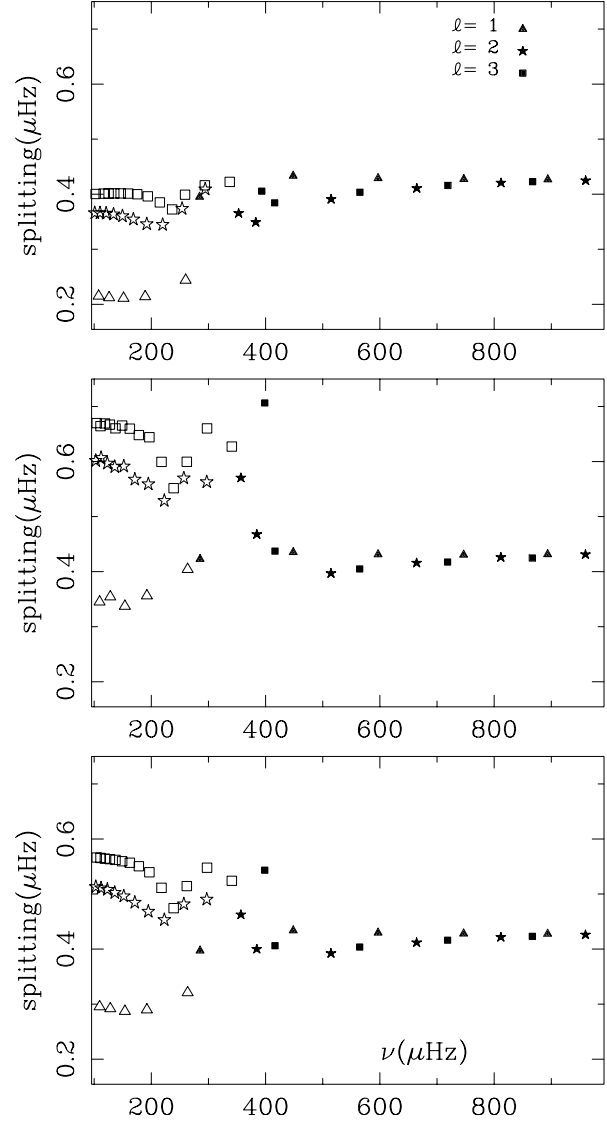


**Fig. 10.** Splittings of low degree low-frequency  $\ell = m$  modes as a function of the frequency for the reference model M1 and for the simplified rotation law described in the text for  $r > 0.2 R_\odot$  and different rotation laws below  $0.2 R_\odot$ . Upper panel: Simplified rotation law as described in the text with  $\Omega_c = 0.433 \mu\text{Hz}$ . Middle panel:  $\Omega = 2\Omega_c$  for  $r < 0.2 R_\odot$ . Lower panel: linear central rotation, increasing from  $0.433 \mu\text{Hz}$  at  $0.2 R_\odot$  to  $0.833 \mu\text{Hz}$  at the center of the model ( $\Omega = \Omega_c(2 - r/0.2R_\odot)$ ). Open (*resp.* full) symbols for g- (*resp.* f- and p-) modes.

As the low-frequency oscillations have a large amplitude in the solar core, their splittings are particularly sensitive to the rotation close to the center, which is up to now poorly known. In order to investigate the behavior of these splittings relatively to the frequency and the degree, we have used a simplified rotation law, as follows. For  $r \geq 0.4 R_\odot$  we approach the rotation rate obtained by inversion from the p-mode data, i.e. rigid rotation below the convection zone and differential rotation inside (see e.g. Corbard et al. 1997):

$$\text{for } 0.7 < r/R_\odot < 1, \quad \Omega = \Omega_0 + \Omega_1 \cos^2 \theta + \Omega_2 \cos^4 \theta,$$

with  $\Omega_0 = 454$  nHz,  $\Omega_1 = -54.6$  nHz and  $\Omega_2 = -75.4$  nHz;

for  $0.4 < r/R_\odot < 0.7$ ,  $\Omega = 433$  nHz.

As the core rotation remains more uncertain, we assume that it has a constant value equal to  $\Omega_c$ .

Let us recall that for a rigid rotation  $\Omega$  the mode splitting can be written, using Ledoux (1951):

$$\sigma_{n,\ell,m} = \Omega(1 - C_{n,\ell}).$$

$C_{n,\ell}$  is small compared to 1 for p-modes and asymptotically equal to  $1/\ell(\ell+1)$  for g-modes. For the simplified solar rotation law considered here, the results are given for the splittings  $\sigma_{n,\ell,\ell}$  of the sectoral modes in Fig. 10 (upper panel). They do not depend very much on the details of the rotation law. It can be shown, indeed, that in the considered frequency range a rigid rotation of  $0.433$   $\mu$ Hz in the whole Sun will change the g-mode splittings by less than  $0.5$  nHz and the p-mode splittings by  $2$  to  $7$  nHz. At low frequency, the splittings of the modes of degree  $\ell=1, 2$  and  $3$  are very different according the degree  $\ell$  with a behavior close to the asymptotic behavior of g-modes, i.e. a splitting proportional to  $1 - 1/\ell(\ell+1)$ . At high frequencies the splittings have the asymptotic p-modes values, with a very weak dependence on the degree  $\ell$  due to the differential rotation in the convection zone. They are systematically slightly larger for  $\ell=1$  p-modes. In the mixed modes frequency range  $200 - 400$   $\mu$ Hz, the splittings vary significantly with the degree and frequency.

In order to point out the sensitivity of the low-frequency splittings to the solar core rotation, we have computed them for two other rotation laws below  $0.2 R_\odot$ :  $\Omega = 2\Omega_c$  and  $\Omega = \Omega_c(2 - r/0.2R_\odot)$ . For  $r > 0.2R_\odot$ , we keep the previous rotation law. In the middle (*resp.* lower) panel of Fig. 10, we have plotted the splittings for these two rotation laws. As expected the g-mode splittings are significantly increased by about a factor  $1.7$  (respectively  $1.45$ ) while the p-mode splittings are almost unchanged. Note, from the comparison of Fig. 10, upper and middle panels, the large increase of splitting of the f-modes ( $\ell=2$  and  $3$ ), due to the behavior of their eigenfunctions, which are peaked in the solar core, like the f-mode ( $\ell=6$ ) given in Fig. 3. (Let us recall, that, for  $\ell=1$ , the f-mode does not exist.) The splittings of the mixed modes have a complex dependence on degree, frequency and shape of the rotation law below  $0.2 R_\odot$ . If the rotation of the solar core differs notably from that of the radiative zone, such a behavior will make their detection and identification in the observed spectrum harder.

## 6. Conclusions

In this paper we have studied the properties of solar low-frequency oscillations and their sensitivity to the physics of the solar interior. A set of solar models with different age, metallicity, luminosity and updated nuclear reaction rates and involving several physical processes like overshoot, mass loss and mixing below the convection zone, has been computed. In order to help the detection of g-modes with the LOI instrument, we have considered low-frequency modes of degrees  $\ell$  up to  $6$ .

We have pointed out the existence of a set of modes with frequencies around  $280$   $\mu$ Hz which have a mixed character, i.e. they have noticeable amplitude both in the core and in the surface layers. These mixed modes lie in the region of the avoided crossing of g-modes with the f-mode ridge. Their inertia is smaller than the inertia of the neighbouring modes, which makes them easier to excite. If we assume that the excitation mechanism given by Kumar et al. (1996) is not too sensitive to the degree, some g-modes especially of degree  $\ell=4, 5$  and  $6$  could have same observable amplitudes than the first g-modes of low degree, i.e.  $0.1$  mm s<sup>-1</sup>.

We have shown that the rotational splittings of the modes for  $\nu < 400$   $\mu$ Hz are very sensitive to the up to now unknown solar core rotation. Unlike the p- ( $\nu > 400$   $\mu$ Hz) and g-mode ( $\nu < 200$   $\mu$ Hz) splittings, which are well described by asymptotic approximations, the mixed modes in the frequency range  $200 - 400$   $\mu$ Hz have splittings very sensitive to degree and frequency. The prediction of these splittings in view of detection of these modes in the low-frequency spectrum is thus very delicate and dependent on the solar core rotation.

We have considered the sensitivity of the low-frequency modes to the physics and ingredients of the models. As expected, in the considered frequency range, the frequencies of p-modes for degrees  $\ell \leq 6$  vary very little with the model. In contrast we have shown that the sensitivity of g-, f- and p<sub>1</sub> modes is large below  $400$   $\mu$ Hz. Their frequencies increase with the age, the photospheric metallicity, and if mass loss occurs during the beginning of solar evolution. They are decreased if there is some convective core overshoot in the early evolution. Thus the observation of the modes below  $400$   $\mu$ Hz will be important to constrain the solar model. We pointed out that the mixed modes have a sensitivity smaller, but still larger than the one of low-frequency p-modes. The results of our calculations show that they are in the frequency range  $200 - 400$   $\mu$ Hz the most promising modes to be detected.

*Acknowledgements.* The authors thank the referee for constructive comments. This work has been partly performed using the computing facilities provided by the OCA program ‘‘Simulations Interactives et Visualisation en Astronomie et M canique (SIVAM)’’.

## References

- Adelberger E., Austin S.M., Bahcall J.N., et al., 1998, Rev. Mod. Phys. 70, 4, 1265
- Bahcall J.N., 1997, Phys. Rev. C 56, N6, 3391
- Bahcall J.N., Lisi E., Alburger D.E., et al., 1996, Phys. Rev. C 54, 411
- Basu S., 1997, In: Provost J., Schmider F.X. (eds.) Sounding solar and stellar interiors. IAU Symposium 181, Kluwer Academic Publishers, p. 137
- Basu S., Antia H.M., 1995, MNRAS 276, 1402
- Berthomieu G., Provost J., 1991, Solar Phys. 133, 127
- Brun S., Turck-Chi ze S., Zahn J.P., 1998, In: Wilson A., Korzennick (eds.) SOHO6/GONG98: Structure and Dynamics of the Interior of the Sun and Sun-like Stars. ESA Publication SP-418, p. 439
- Caughlan G.R., Fowler W.A., 1988, Atomic Data and Nuclear Data Tables 40, 284

- Christensen-Dalsgaard J., Berthomieu G., 1991, In: Cox A.N., Livingston W.C., Matthews M. (eds.) *Solar interior and atmosphere*. University of Arizona Press, p. 401
- Christensen-Dalsgaard J., Däppen W., Antia H.M., et al., 1996, *Sci* 272, 1286
- Corbard Th., Berthomieu G., Morel P., et al., 1997, *A&A* 324, 298
- Davis R. Jr., 1994, *Prog. Part. Nucl.* 32, 13
- Dziembowski W.A., Fiorentini G., Ricci B., Sienkiewicz R., 1999, *A&A* 343, 990
- Ellis A.N., 1986, In: Gough D.O. (ed.) *Seismology of the Sun and the Distant Stars*. Reidel Publishing Company, Dordrecht, p. 173
- Fröhlich C., Andersen B., Appourchaux Th., et al., 1997 *Solar Phys.* 170, 1
- Fröhlich C., Finsterle W., Andersen B., et al., 1998, In: Wilson A., Korzenick (eds.) *SOHO6/GONG98: Structure and Dynamics of the Interior of the Sun and Sun-like Stars*. ESA Publication SP-418, p. 67
- Fukuda Y., Kamiokande Collaboration, 1996, *Phys. Rev. Lett.* 77, 1683
- Gabriel M., 1986, In: Gough D.O. (ed.) *Seismology of the Sun and the Distant Stars*. Reidel Publishing Company, p. 177
- Gabriel A., Turck-Chièze S., Garcia R., et al., 1998, In: Wilson A., Korzenick (eds.) *SOHO6/GONG98: Structure and Dynamics of the Interior of the Sun and Sun-like Stars*. ESA Publication SP-418, p. 61
- Gough D.O., Kosovichev A.G., Toomre J., et al., 1996, *Sci* 272, 1296
- Grevesse N., Noels A., 1993, In: Prantzos N., Vangioni-Flam E., Cassé M. (eds.) *Origin and evolution of the elements*. Cambridge University Press, p. 15
- Grevesse N., Sauval A.J., 1998, *Space Sci. Rev.* 85, 161
- Guenther D.B., Demarque P., Kim Y.C., Pinsonneault M.H., 1992, *ApJ* 387, 372
- Guzik J.A., Cox A.N., 1995, *ApJ* 448, 905
- Hampel W., Handt J., Heusser G., GALLEX collaboration, 1999, *Phys. Lett. B* 447, 127
- Kippenhahn R., Weigert A., 1991, *Stellar Structure and Evolution*. Springer Verlag, Berlin, Heidelberg, New York, (Sect. 28.2)
- Kumar P., Quataert E.J., Bahcall J.N., 1996, *ApJ* 458, L83
- Lazrek M., Baudin F., Bertello L., et al., 1997, *Solar Phys.* 175, 227
- Ledoux P., 1951, *ApJ* 114, 373
- Montalban J., Schatzman E., 1999, *A&A* in press
- Morel P., Provost J., Berthomieu G., 1997, *A&A* 327, 349
- Morel P., Provost J., Berthomieu G., 1998a, In: Wilson A., Korzenick (eds.) *SOHO6/GONG98: Structure and Dynamics of the Interior of the Sun and Sun-like Stars*. ESA Publication SP-418, p. 499
- Morel P., Provost J., Berthomieu G., Audard N., 1998b, In: Provost J., Schmider F.X. (eds.) *Sounding solar and stellar interiors*. poster volume, OCA & UNSA, p. 109
- Morel P., Pichon B., Provost J., Berthomieu G., 1999 *A&A* 350, 275
- Provost J., Berthomieu G., 1986, *A&A* 165, 218
- Provost J., Berthomieu G., Morel P., 1998, *Space Sci. Rev.* 85, 117
- Richard O., Vauclair S., Charbonnel C., Dziembowski W.A., 1996, *A&A* 312, 1000
- Tassoul M., 1980, *ApJS* 43, 457
- Turck-Chièze S., Basu S., Brun S., et al., 1997, *Solar Phys.* 175, 247